The research of the effectiveness of the ice cover destruction by the resonance method from the pair motion of the load

V L Zemlyak[1], E G Rogozhnikova[2], A S Vasilyev[1] and S V Radionov[1]

[1] Sholom-Aleichem Priamursky State University, 70a Shirokaja Street, Birobidzhan, 679015, Russia

[2] Amur State University of Humanities and Pedagogy, 17/2 Kirova Street, Komsomolsk-on-Amur, 681000, Russia

vellkom@list.ru

Abstract. In the work, the efficiency of study of the ice cover by the resonant method from the pair movement of the load is experimentally investigated. Studies were conducted in the experimental ice tank. At the initial stage of the study, a series of experiments was conducted to determine the effect of the mass of the load on the parameters of flexural-gravity waves generated in model ice. Further, the effect of the distance between the load models during their pair wake movement was studied. Study have shown that, depending on the distance between the models, either an increase or a decrease in the effectiveness of ice cover destruction was observed by flexural-gravity waves, which is associated with the interference phenomenon — an increase and decrease in the resulting amplitude of two coherent wave systems generated from the motion of the models. In general, it can be concluded that, to increase the efficiency of the resonant method of breaking the ice, flexural-gravity waves can be used as repeated passes of a single load across the ice cover, as well as pair movement.

1. Introduction

Working out of coastal and shelf areas under the frozen seashore sea is associated with the problem of ice cover failure. There are various methods and technical means for failure the ice cover. One of these methods is the failure of the ice cover by flexural-gravitational waves (FGW) when the loads moves on the ice cover. One such load is an air cushion vehicles (ACV). Their excellent maneuverability, super cross-country ability and independence from the depth of the pool, let us apply to them under conditions when large icebreakers are useless.

Single load motion has been reviewed in [1, 2, 3]. The load movement along an ice cover with varying basin depth in the case of a two-dimensional problem was considered in [4]. The study on the plane problem about the influence of periodic external load on the oscillations of a semi-infinite elastic plate and a strip was described in [5]. The theoretical study of stationary and nonstationary load movement on an ice cover is described in [6], and the experimental research on the deformation of an ice cover with a load moving on it is given in [7]. The destruction of ice by dynamic loads is considered in the work [8].

However, during the implementation of ice breaking works by single ACV, ACV parameters may appear insufficient for failure of the ice cover of specified thickness at specific ice conditions. In these cases, efficiency of ice breaking works may be increased by simultaneous use of several hovercrafts, i.e. by interference of FGW generated by ACV. This work is dedicated to research of the ice cover deformation during the motion of paired loads over it.

2. Equipment and technique for conducting experiments

Experimental research of the ice cover deformation during the motion of paired loads over out in the ice tank of the Ice Technology Laboratory of Sholom-Aleichem Priamursky State University (Birobidzhan, Russia) [9]. The dimensions of the ice tank are 14×3×1 m.

A simplified model of ACV Murena (scale 1:60) is used for the experiments. The model is fabricated with 3D printer using layer-by-layer technique (Figure 1). The model length is $l_m = 0.5$ m; the model width is $b_m = 0.216$ m; the model weight is $m_m = 0.94$ kg. The speed is $u_m = 1.4 \div 2.2$ m/s. The same parameters of the model are used for theoretical calculations.

The ice cover model is made in the ice tank by freezing natural freshwater of the set thickness (0.002 m) without any impurity in natural conditions.
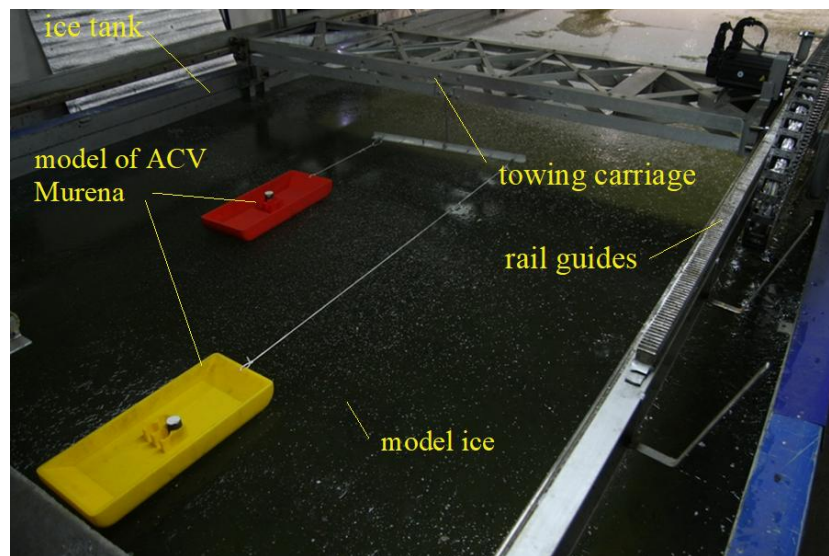
Figure 1. Load models before the start of experiments.

Modeling of ice cover can be executed by using various ice models and for each of them there are corresponding conditions of similarity. The usual modeling is performed with partial satisfaction of conditions of similarity [10].

When the natural ice cover is used as a model one, the thickness of the modelled ice will be calculated when converted to a full-scale one in accordance with the following relations:

$$h_n = h_m \lambda_l^{4/3} \left(\frac{[\sigma_u]_n}{[\sigma_u]_m} \right)^{-\frac{1}{3}}$$

Where h_n is the natural ice thickness; h_m is the modeled ice thickness; $[\sigma_u]_n$ is the natural flexural stresses; $[\sigma_u]_m$ is the modeled flexural stresses.

The determination of the flexural strength of the modelled ice is experimentally performed by testing beams afloat [11] for that purpose the modelled ice cover is prepared by building up the ice of the required thickness h_m=0.002 m, $[\sigma_u]_m = 1.53 \cdot 10^6$ Pa. The value of the flexural strength of the freshwater ice $[\sigma_u]_n = 0.7 \cdot 10^6$ Pa is chosen according to the work Petrov [12]. The thickness of the modelled ice cover after conversion to a natural one is h_n=0.6 m.

It is known that when modelling sea ice by using fresh-water modelled ice, the elasticity modulus of natural ice should be less than the elasticity modulus of modelled ice $E_n > E_m$, however the ratio E/σ_u for sea ice is practically the same as that for fresh-water ice. To meet this condition in modelling ice is very important [13].

The stages of ice destruction can be estimated using geometric characteristics. Studies make it possible to determine the minimum angle of the tangent inclination to the deformed surface, sufficient for complete destruction of the ice during bending. The results show that the slope should not be less

than 15^0. Then, as a parameter for the complete destruction of the solid ice cover, we can take the value of the angle of the tangent inclination to the curved surface of the ice plate, characterizing the curvature of the FGW and equal to:

$$\alpha = 2\pi w_m / \lambda_m$$

The dependence between the failure of the ice cover and the coefficient α has already been determined in work [14]. These model experiments on the failure of the natural ice cover of various thicknesses are conducted using of submarine models and hovercrafts. It is found, that for the load motion on the ice cover as well as for the submarine motion, when the maximum value of the slope of the ice surface exceeds the value of 0.04, it causes complete ice failure and crack opening.

3. The numerical model

Theoretical research of effect of mutual location of air cushion ships on the parameters of FGW generated by them has been performed based on solution of differential equation of small oscillation of floating visco-elastic plate under effect of external load that may be written as follows [1]:

$$\frac{Gh^3}{3}\left(1 - \tau_\varphi u \frac{\partial}{\partial x}\right)\nabla^4 w + \rho_1 g w + \rho_2 h u^2 \frac{\partial^2 w}{\partial x^2} - \rho_1 u \frac{\partial \Phi}{\partial x} = -q \tag{1}$$

Where G is modulus of ice elasticity during the shift; $G = 0.5E/(1+\nu)$; h is ice cover thickness; τ_φ is time of deformation relaxation; w is ice sagging; ρ_1 is ice plate density; ρ_2 is water density; g is acceleration of gravity; u is speed of load motion; q is system of moving pressures; Φ is motion potential of liquid consistent with Laplace equation $\Delta\Phi = 0$.

Expression for w is obtained in form of:

$$w(x,y) = \frac{4q_0}{\pi^2 \cdot \rho_1 \cdot u^2} \cdot \int_0^\infty \lambda^2 \cdot \tanh(\lambda H) \times$$

$$\times \int_0^\lambda \frac{\cos\left(y\sqrt{\lambda^2 - \alpha^2}\right)\sin\left(\alpha\frac{l_n}{2}\right)\sin\left(\frac{b_n}{2}\sqrt{\lambda^2 - \alpha^2}\right)(\cos(\alpha x)\cdot\xi + \sin(\alpha x)\cdot\eta)}{\alpha(\lambda^2 - \alpha^2)(\xi^2 + \eta^2)} d\alpha d\lambda \tag{2}$$

where

$$\xi = -\frac{Gh^3\lambda^5 \tanh(\lambda H)}{3\rho_1 u^2} - \frac{g\lambda \tanh(\lambda H)}{u^2} + \frac{\rho_2 h\lambda\alpha^2 \tanh(\lambda H)}{\rho_1} + \alpha^2 \tag{3}$$

$$\eta = \frac{Gh^3\lambda^5 \tanh(\lambda H)\alpha\tau_\varphi}{3\rho_1 u} \tag{4}$$

Where q_0 is load intensity; l_n is load length; b_n is load width; H is water depth.

In order to determine total theoretical sagging of an ice cover during the motion of two loads upon it, following dependences were used:

$$w_f(x,y) = w(x,y) + w(x, y - L_Y) \tag{5}$$

$$w_k(x,y) = w(x,y) + w(x + L_X, y) \tag{6}$$

Where: L_Y is distance between loads during their motion in side-by-side; L_X is distance between loads during their motion in a single column.

The stress-strain properties of ice are: $E = 1\cdot10^6$ Pa; $\mu = 0.33$; $\tau_\varphi = 0.69$ s; $\rho_1 = 900$ kg/m^3; $\rho_2 = 1000$ kg/m^3.

4. Single moving load

In order to verify the proposed mathematical algorithm, the results of simulated experiments performed in experimental ice basin are compared with theoretical calculation data for a single moving load. The results are shown in Figure 2 as ice cover deflection and in Figure 3 FGW length vs. load speed curve. It should be noted that during the simulated experiments we did not observe failure of the ice cover. These load properties are selected in order to determine the most favorable movement modes at the next stage, which would cause ice failure due to interference of FGW.
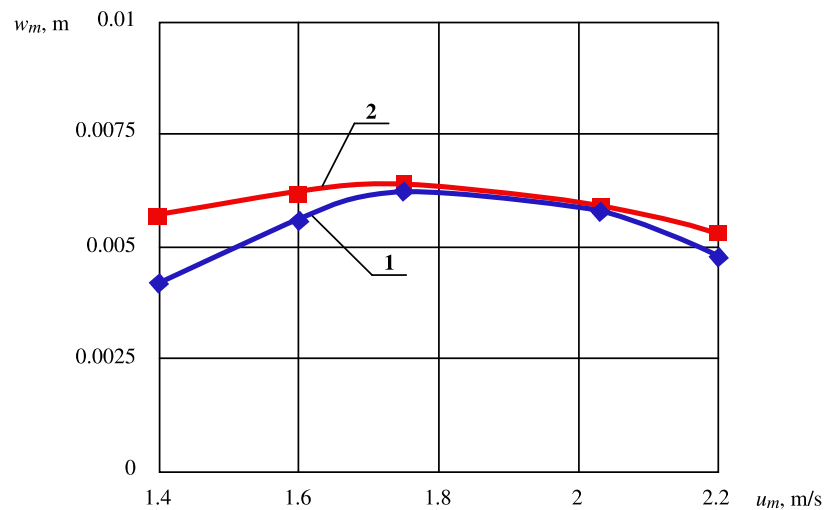
Figure 2. Dependence of the deflections of the model ice (h_m=0.002 m) on the motion speed of the load weights m_m=0.94 kg: *No.1* experimental results; *No.2* calculated theoretical results.
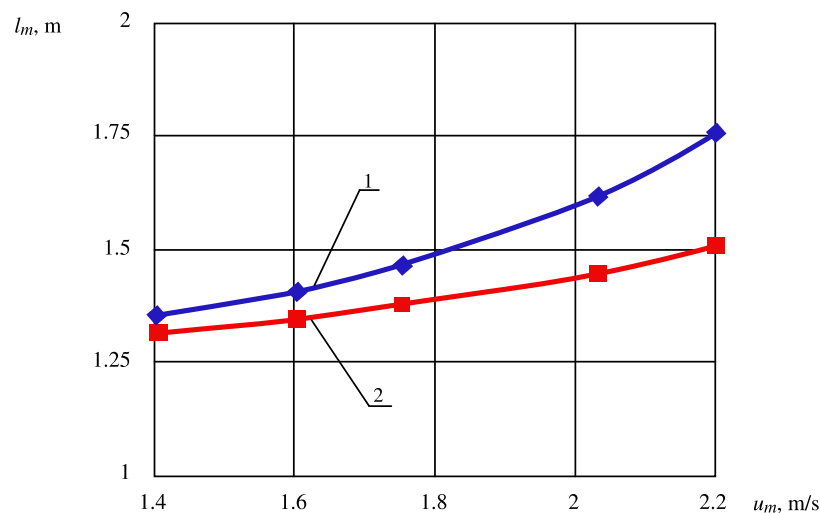
Figure 3. Dependence of the length FGW of the model ice (h_m=0.002 m) on the motion speed of the load weights m_m=0.94 kg: *No.1* experimental results; *No.2* calculated theoretical results.

Resonant speed of the load determined using the highest ice cover deflections is approx 1.75 m/s. Comparison of FGW parameters obtained by simulated experiments and theoretical calculations shows that maximum difference between the ice deflections and FGW lengths obtained at critical speed of u_m=1.75 m/s is 3% and 6%, accordingly.

Generally, we can conclude that the mathematical algorithm proposed shows that both qualitative and quantitative results of theoretical calculations and experiments for destruction of natural ice by FGWs match each other. Only for low speeds, the difference between the results achieves 27% due to technical difficulties encountered during experiments at speeds below 1.5 m/sec and difficult preparation of the simulated ice field with the specified physical and mechanical properties.

5. The movement of the pair loads

5.1. Movement of models side-by-side formation

The experiments performed Kozin [7] show that ice cover can be fractured by FGW with higher efficiency if the loads are moving in pair. In order to obtain the parameters of the FGW being generated, a number of experiments is performed where air-cushion ships are moving in side-by-side formation and in a single column formation.

The distance between the models moving in side-by-side formation varied from zero to $2b_m$. The experiment layout showing location of sensors, length of acceleration section and stationary motion section is shown in Figure 4. All dimensions of the models are in meters. Schemes experiment were made in AutoCAD 2019.
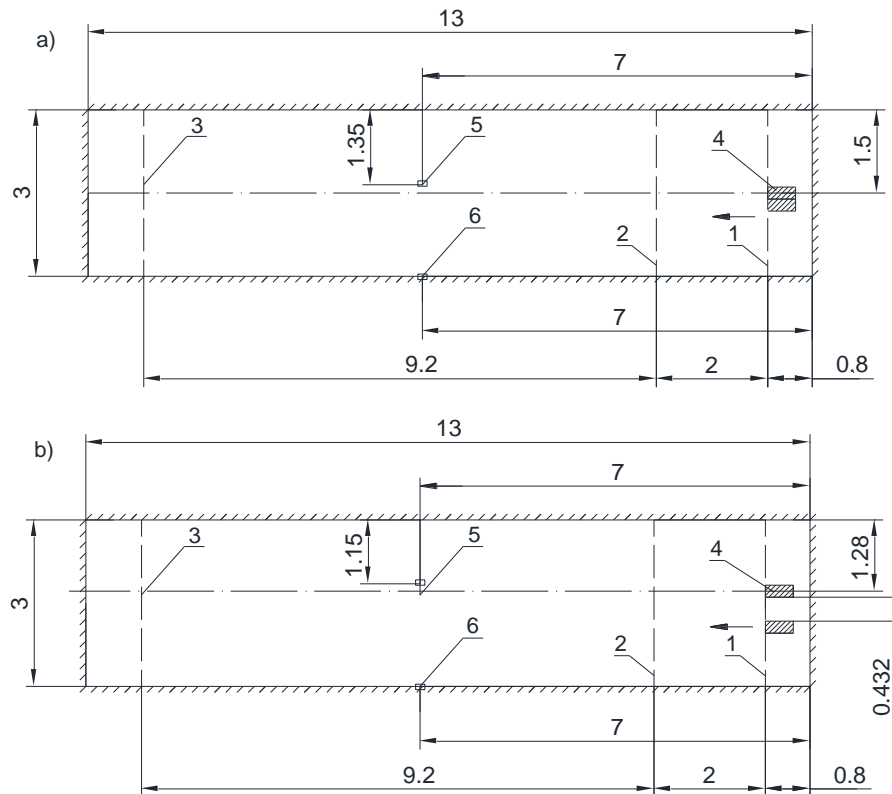

Figure 4. Schemes experiment (a – zero distance between models, b – distance between models is $2b_m$)): 1 model motion start line; 2 acceleration section end line; 3 – stationary motion section end line; 4 model of ACV Murena; 5 motion sensor; 6 speed sensor.

Highest deflections and coefficient α are observed at load speed of u_m=1.75 m/s. The larger the distance between the models, the lower the ice-fracturing capacity of FGWs. In experiments and theoretical calculations, if the distance is b_m, the average ice deflections are 24% lower, and the average coefficient α is 22% lower. If the distance is $2b_m$ – 35% and 40% lower, accordingly (Figures 5-6).
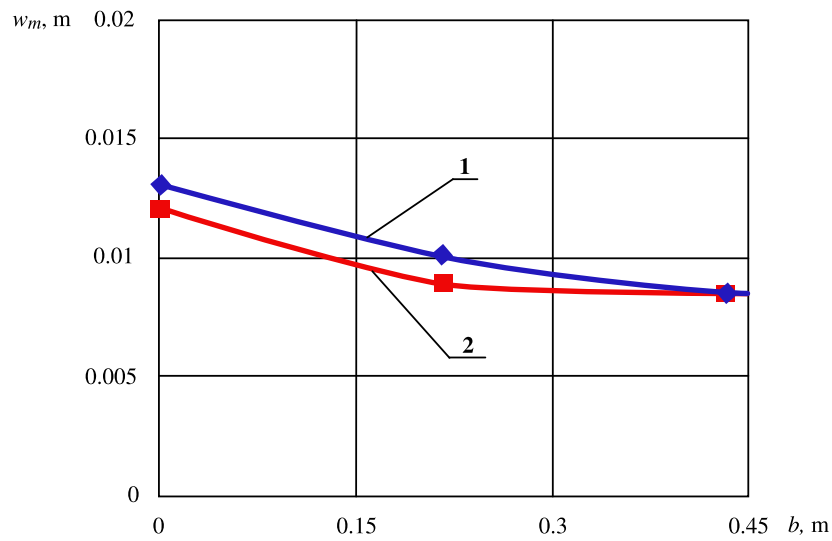
Figure 5. Maximum ice plate deflection (h_m = 0.002 m) vs distance between loads for speed of u_m=1.75 m/s: *No.1* experimental results; *No.2* calculated theoretical result.
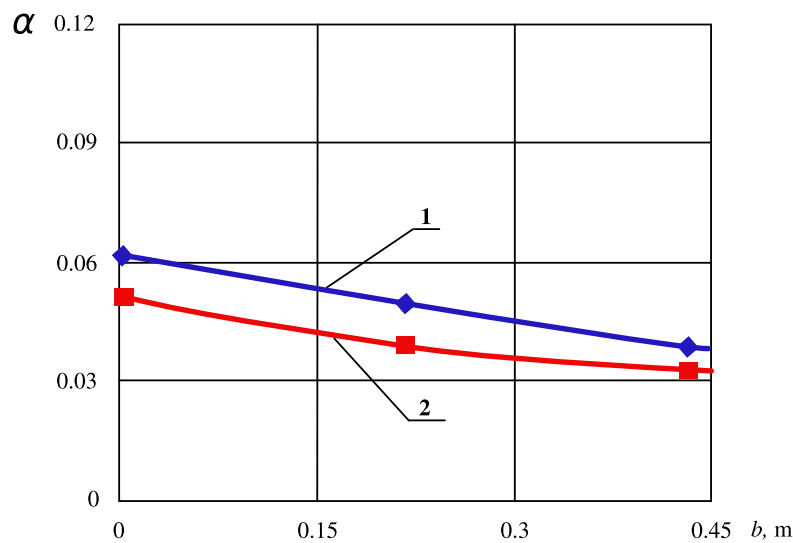

Figure 6. Coefficient α of the ice plate (h_m = 0.002 m) vs distance between loads for speed u_m=1.75 m/s: *No.1* experimental results; *No.2* calculated theoretical result.

Difference between the compared theoretical calculations and experimental data is adequately low. Only in some cases, the difference reached 23% (table 1).

Table 1. Comparison between data of simulated experiments and theoretical calculations for models moving in side-by-side formation.

Distance between loads (m)	Speed (m/s)	Deflection (m)		FGW length (m)	
		experimental	theoretical	experimental	theoretical
Zero distance between models	1.4	0.0085	0.0091	1.12	1.31
	1.6	0.01	0.01	1.28	1.38
	1.75	0.013	0.012	1.31	1.45
	1.96	0.0126	0.0097	1.37	1.51
	2.17	0.0091	0.0087	1.73	1.7
0.216	1.4	0.0078	0.0067	1.26	1.32
	1.57	0.0085	0.0077	1.32	1.38
	1.75	0.01	0.0089	1.36	1.4
	2	0.009	0.0073	1.4	1.42
	2.17	0.007	0.0065	1.73	1.72
0.432	1.4	0.0067	0.0061	1.3	1.25
	1.57	0.007	0.007	1.35	1.32
	1.75	0.0085	0.0075	1.4	1.41
	2.03	0.0069	0.0065	1.82	1.5
	2.25	0.0045	0.0057	2.25	1.8

During the experiments, at the critical speed, dense cracks are observed, ice cover loses its load bearing capacity, ice pieces are chipped and overturned. The ice was fractured over the significant area and directly under the models (Figure 7). As the speed increases, the fracture efficiency decreases and ice cracking pattern changes. The cracks are caused by divergent waves (Figure 8).
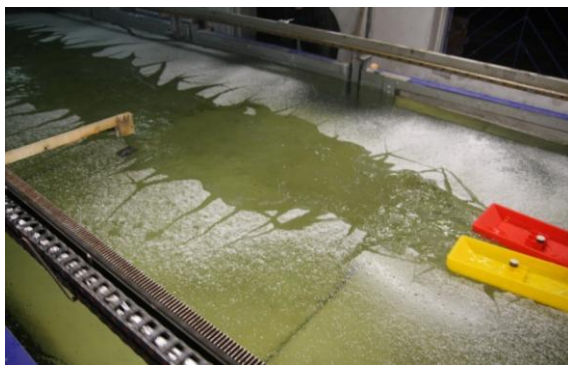
Figure 7. Ice model fraction pattern (h_m = 0.002 m) caused by FGW generated by models moving in side-by-side formation at speed of u_m = 1.75 m/s with zero distance between them.
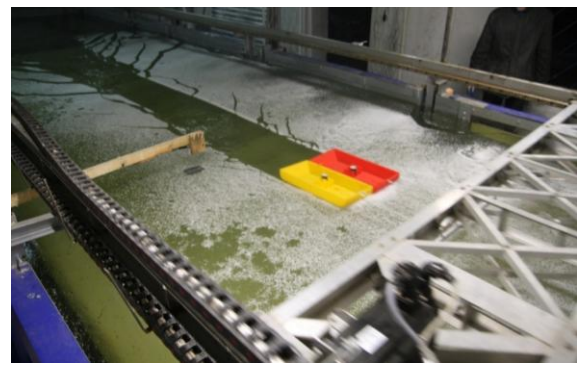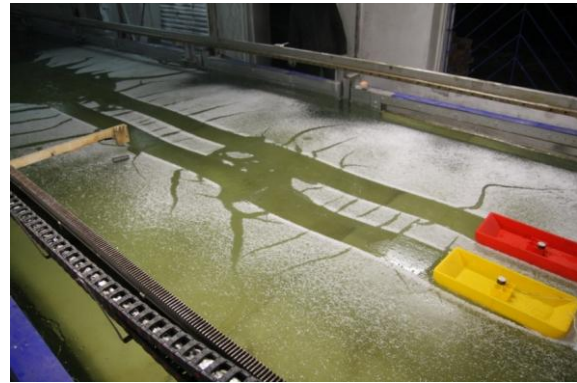

Figure 8. Ice model fraction pattern (h_m = 0.002 m) caused by FGW generated by models moving in side-by-side formation at speed of u_m = 1.96 m/s with zero distance between them.

The greater the distance between the models, the lower their ice fracturing capacity at the same speed. The lowest deflections observed are caused by models moving in side-by-side formation at the distance of $2b_m$ from each other (Figures 9-11).

Figure 9. Ice model fraction pattern (h_m = 0.002 m) caused by FGW generated by models moving in side-by-side formation at speed of u_m = 1.57 m/s with zero distance between them [15].

Figure 10. Ice model fraction pattern (h_m = 0.002 m) caused by FGW generated by models moving in side-by-side formation at speed of u_m = 1.57 m/s with the distance between them equal to b_m [15].


Figure 11. Ice model fraction pattern (h_m = 0.002 m) caused by FGW generated by models moving in side-by-side formation at speed of u_m = 1.57 m/s with the distance between them equal to $2b_m$ [15].

Ice fracture with complete loss of load bearing capacity is not observed. If the speed is close to critical value, main cracks are generated in the ice, but not expanded completely (Figure 11). FGW period is higher; curvature is significantly lower.

5.2. Movement of models by line ahead

The further study covered the effects caused by distance between the pair of models of ACV Murena moving by line ahead (Figure 12). Distance between the models varied from zero to $2l_m$ (a greater distance makes no sense due to almost complete attenuation of FGW generated by the first model). Model parameters and their speeds are the same as those in previous experiments. All dimensions of the models are in meters. Schemes experiment were made in AutoCAD 2019.
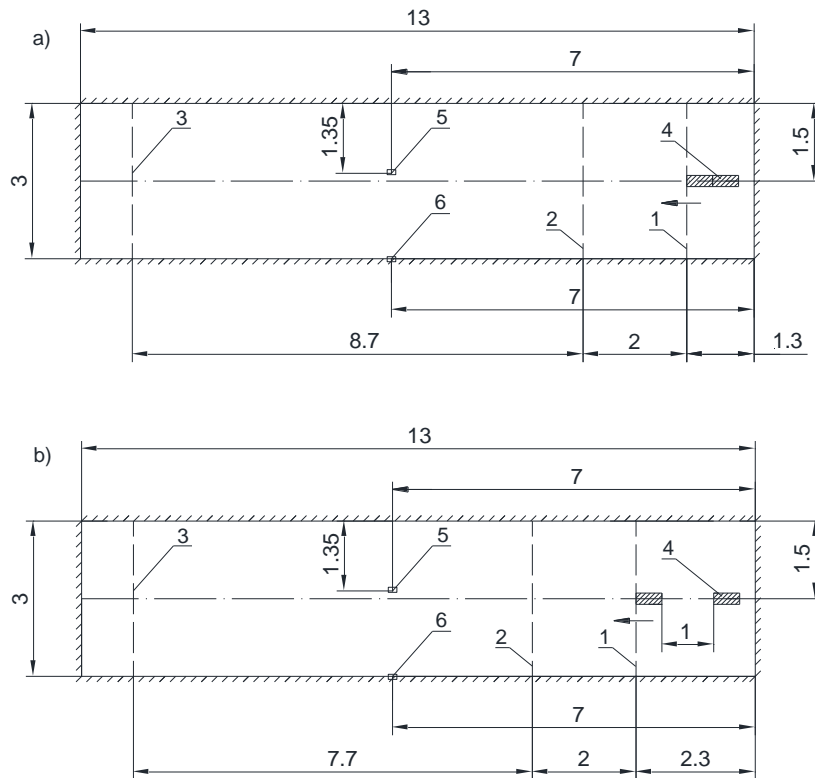
Figure 12. Schemes experiment (a – zero distance between models, b – distance between models is $2l_m$)): 1 model motion start line; 2 acceleration section end line; 3 stationary motion section end line; 4 model of ACV Murena; 5 motion sensor; 6 speed sensor.

Calculation and experiment results are shown in table 2. Comparison of deflections caused by loads moving in a single column formation shows differences up to 35%. When the load speed is close to the critical speed, the difference is much lower and not exceeding 18%. Generally, we can make a conclusion that we should know the exact physical and mechanical properties of the ice model for each individual simulation case in order to decrease the difference between experimental and theoretical data, since the maximum error at some points is 2%. FGW length data is satisfactory. The maximum average difference between the values is 15%.

The highest deflections, as in the above cases, are observed at the load speed of u_m=1.75 m/s (Figure 13). The study shows that the ice-fracturing efficiency of the paired air cushion ships moving in a single column formation is low (Figure 14). Coefficient α are much lower than minimum value of 0.04, at which formation of expanded cracks is observed in the experiments. Even in the best case, when speed reached the critical value and distance between the loads is $l = 0.5$ m, the ice-fracturing capacity of FGWs was insufficient to initiate failure of ice cover with the specified physical and mechanical properties.

Depending on the distance between the models, we observed either increase or decrease in the ice-fracturing efficiency of flexural-gravity waves. The highest deflections are recorded when the distance between the moving loads is $0.5l_m$. In the same case, we observed the highest ice-fracturing capacity of FGWs. If the distance between the models is zero, ice deflection is high enough. However, finally the paired load is a longer single load, which results in significantly greater FGW period and length and lower ice-fracturing capacity of FGW, which is lowest amongst all simulated conditions.

Table 2. Comparison between data of simulated experiments and theoretical calculations for models moving in a single column formation.

Distance between loads (m)	Speed (m/s)	Deflection (m)		FGW length (m)	
		experimental	theoretical	experimental	theoretical
Zero distance between models	1.4	0.0046	0.007	1.6	1.65
	1.53	0.005	0.0082	1.82	1.8
	1.75	0.007	0.0085	1.925	1.89
	2.03	0.0062	0.007	2.03	2
	2.2	0.005	0.0065	2.15	2.1
0.25	1.4	0.005	0.005	1.12	1.45
	1.6	0.0068	0.0057	1.4	1.6
	1.75	0.0075	0.0066	1.5	1.75
	2	0.007	0.0052	1.65	1.9
	2.2	0.006	0.0049	1.98	2
0.5	1.4	0.0035	0.0054	1.18	1.12
	1.57	0.0048	0.0059	1.26	1.125
	1.75	0.0063	0.0062	1.32	1.143
	1.96	0.0053	0.0055	1.37	1.2
	2.1	0.004	0.005	1.89	1.3
0.75	1.36	0.0039	0.0063	1.08	1.13
	1.57	0.0055	0.0064	1.1	1.18
	1.75	0.0062	0.0066	1.225	1.2
	2	0.0042	0.0059	1.6	1.3
	2.2	0.0038	0.0053	1.98	1.4
1.00	1.36	0.0035	0.006	1.36	1.3
	1.57	0.005	0.007	1.41	1.42
	1.8	0.0058	0.0073	1.44	1.6
	1.96	0.0048	0.0059	1.568	1.7
	2.17	0.0041	0.0053	1.736	1.79

The farther the distance between the models, the lower the deflections. Lowest deflections are recorded for the distance of $2l_m$. Increase and decrease in the simulated ice deflections is associated with interference – increase and decrease in resultant amplitude of two coherent FGW systems generated by the moving models.
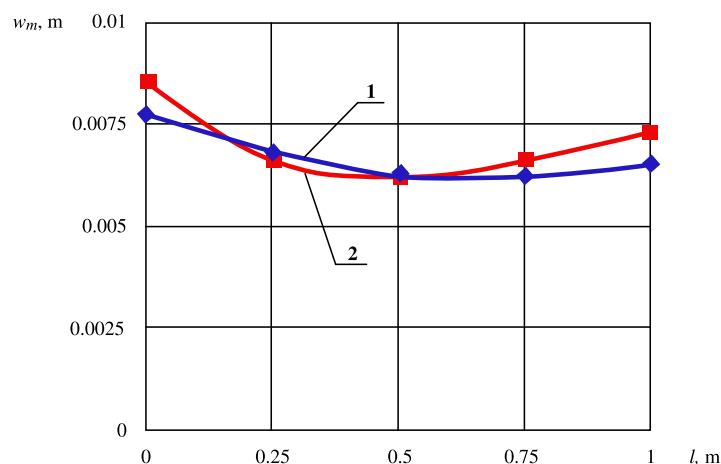
Figure 13. Maximum ice plate deflection ($h_m = 0.002$ m) vs distance between loads for speed of u_m=1.75 m/sec: *No.1* experimental results; *No.2* calculated theoretical result.
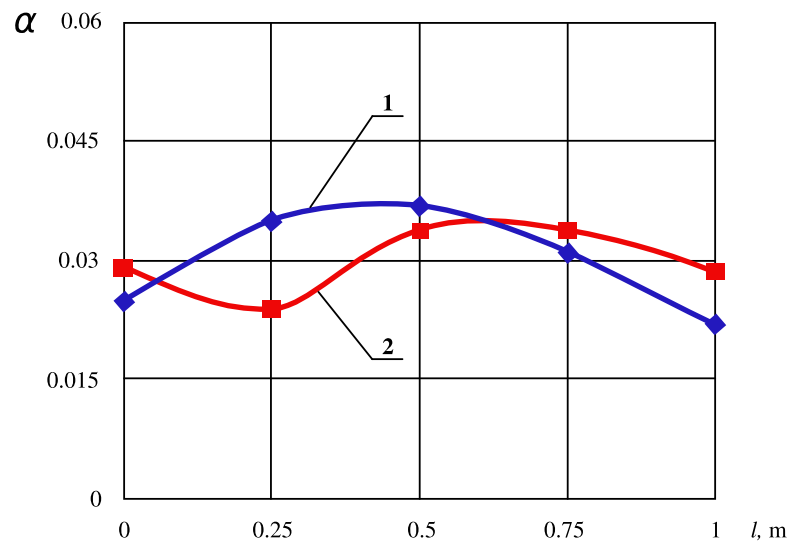
Figure 14. Coefficient α of the ice plate (h_m = 0.002 m) vs distance between loads for speed of u_m=1.75 m/s: *No.1* experimental results; *No.2* calculated theoretical result.

Since the ice cover deflection is lower as the distance between the models grows, ice-fracturing capacity of flexural-gravity waves also becomes lower. This is pronounced most at the critical speeds. On the simulated ice, the ice-fracturing efficiency of FGWs generated by the models moving in a single column formation is extremely low compared to that generated by the models moving in side-by-side formation. Complete loss of load bearing capacity is observed at critical speed only when the distance between models is $0.5l_m$ (Figure 15).

Figure 15. Ice model fracture pattern (h_m = 0.002 m) caused by FGW generated by models moving in a single column formation at speed of u_m = 1.75 m/s with the distance between them equal to $0.5l_m$ [15].

Figure 16. Ice model fracture pattern (h_m = 0.002 m) caused by FGW generated by models moving in a single column formation at speed of u_m = 1.75 m/s with the distance between them equal to l_m.

Figure 17. Ice model fracture pattern ($h_m = 0.002$ m) caused by FGWs generated by models moving in a single column formation at speed of $u_m = 1.75$ m/s with the distance between them equal to $1.5l_m$.

When the distance between the loads grows, the main cracks alone have occurred, but they did not expand, and the load bearing capacity of the ice remained unchanged (Figures 16-17).

6. Conclusion

The experiments have shown that the deflections of the ice cover caused by paired loads of the same weight moving in side-by-side formation at critical speed are 28% to 53% larger than those caused by a single load, and the ice-fracturing capacity of FGW is 30% to 57% higher, depending on distance between the models. Maximum ice-fracturing effect is observed when the distance between the models is zero. The ice cover failed and lost its load bearing capacity almost at each speed used in the study. Failure intensity is lower at supercritical speeds.

For loads moving in a single column formation, the fracture pattern is different. Due to interference of FGWs, the fracturing efficiency either decreased to 23% or increased to 40% as compared with a single load. If the distance between the models is zero, despite the large deflections which are larger than those caused by a single load, ice-fracturing efficiency is extremely low due to the small curvature of FGW.

Generally, we can conclude that both repeated passing of a single load over the ice cover and movement of paired air cushion ships may be used in order to increase the ice-fracturing efficiency of FGW.

The analytical solution proposed shows the satisfactory results. The algorithm is used for prediction of the ice-fracturing capacity of FGW generated by moving paired loads with consideration of performance of the air cushion ships, distance between the ships, their positions relative to each other and physical and mechanical properties of the ice cover (thickness, elastic modulus). Use of the geometrical criterion of complete ice failure in form of the slope of curved surface of ice plate as the ice failure criterion is also acceptable.

Notification
FGW - flexural-gravity waves
ACV - air cushion vehicles

Acknowledgments

References

[1]   Kheisin D E 1967 *Dynamics of Ice Cover* (Gidrometeoizdat: Leningrad) p 216 (in Russian)
[2]   Squire V A, Hosking R J, Kerr A D and Langhorne P J 1996 *Moving Loads on Ice Plates*
        (Kluwer Academic Publishers: Dordrecht) p 236
[3]   Milinazzo F, Shinbrot A and Evans N 1995 *J. Fluid Mech.* **287** 173-197
[4]   Sturova I V 2008 *J. of Appl. Math. Mech.* **72** 588–600
[5]   Tkacheva L A 2004 *J. of Appl. Mech. Tech. Phys.* **45** 420–427
[6]   Wang K, Hosking R J and Milinazzo F 2004 *J. Fluid Mech.* **21** 295–317
[7]   Takizawa T 1985 *Cold Regions Sci. Tech*. **11** 171-180
[8]   Orlov M Yu *et al* 2019 *J. Phys.: Conf. Ser.* **1214** 012001
[9]   Zemlyak V L, Baurin N O and Kurbackiy D A 2013 *Vestnik Quart. J. of Amur State University
        after Sholom-Aleichem* **12** 75–84 (in Russian)
[10] Kozin V M 1983 Substantiation of Initial Data for Choosing Basic Parameters for Hovercraft
        Designed for Breaking Ice Cover by Resonant Method (Gorky Polytechnic Institute after
        Zhdanova) Ph.D. thesis
[11] Stepanjuk I A 2001 *Test Technology and sea ice modeling* (Gidrometeoizdat: St. Petersburg) p
        78 (in Russian)
[12] Petrov I G 1976 *Works of AANII* **331** 4–41 (in Russian)
[13] Lewis J W 1982 *Offshore Technol. Conf*. Houston **4** 493–498
[14] Kozin V M, Onishchuk A G and Mar'in B N 2005 *The Ice-Breaking Capacity of Flexural-Gravity
        Waves Produced by Motion of Objects* (Dal'nauka, Vladivostok) p 191 (in Russian)
[15] Rogozhnikova E G, Kozin V M, Zemlyak V L 2019 *Proc. Int. Conf. ISOPE* (Honolulu, USA)
        729–734